2021

The Role of the Golgi ELMO Proteins in Cell Adhesion in *Arabidopsis thaliana*

Wesley James Hudson
Bowdoin College

The Role of the Golgi ELMO Proteins in Cell Adhesion in *Arabidopsis thaliana*

An Honors Project for the Department of Biology

By Wesley James Hudson

Bowdoin College, 2021

Table of Contents

Acknowledgements

First, I would like to acknowledge and thank Bruce Kohorn. His leadership, guidance, and support this past year have been invaluable in my development as a scientist. I am incredibly thankful to have had the opportunity to pursue this project. Next, I would like to thank Sue Kohorn. This project would not have been possible if not for her support and dedication. I would also like to thank my lab mate Andy Bolender for his positivity and humor. Working alongside Andy brought me immense joy this past year. Further, I would like to thank my friends and family for their endless support throughout my time at Bowdoin. I also would like to thank Barry Logan for his comments and suggestions on this paper, and for his guidance and support throughout my time at Bowdoin. Lastly, I would like to thank the faculty, staff, and students of the Biology Department for their role in my academic and personal growth these past four years.

Abstract

Proper growth and development of plant cells is dependent upon successful cell adhesion between cells, and this is mostly mediated by pectin in the plant cell wall. Previously, the Kohorn Laboratory identified a non-enzymatic Golgi protein named ELMO1 as it is required for cell adhesion, likely acting as a scaffold for cell wall polymer synthesis. Plants with mutant ELMO1 demonstrate a weak defective cellular adhesion phenotype as well as reduced mannose content in the cell wall. ELMO1 has homologous proteins in at least 29 different vascular plants. These homologues have 2 possible deletions in their amino acid sequence, but protein modeling determined that these variations will not affect protein structure. There are 5 homologous ELMO1 proteins in *Arabidopsis thaliana* that have been aptly named ELMO2, ELMO3, ELMO4, ELMO5. *elmo2*$^{-/-}$ mutants revealed no mutant adhesion phenotypes, while *elmo1*$^{-/-}$ *elmo2*$^{-/-}$ double mutants revealed strong defects in adhesion. Confocal microscopy of propidium iodide-stained seedlings confirmed the lack of a phenotype for *elmo2*$^{-/-}$ mutants and showed disorganized gapping cells for the *elmo1*$^{-/-}$*elmo2*$^{-/-}$ mutant. Additionally, while *elmo2*$^{-/-}$ did not have any change to root or hypocotyl length, *elmo1*$^{-/-}$*elmo2*$^{-/-}$ mutants were significantly shorter in both regards. Taken together, these data support that *ELMO2* and *ELMO1* are partially redundant.

Introduction & Background

Plant Cell Wall

The plant cell wall is a complex matrix of polysaccharides and proteins that resides outside of the plasma membrane of plant cells. A number of polysaccharides including cellulose, hemicellulose and pectin are layered in a mesh along with numerous proteins to make up the plant cell wall (Keegstra, 2010). The cell wall is described as having several parts, including the middle lamella and the primary cell wall, both of which play critical roles in plant growth.

Middle Lamella

The middle lamella is an approximately 50 nm thick region between plant cells that contributes to cellular adhesion (Zamil & Geitmann, 2017). The main polysaccharide in the middle lamella is a galacturonic acid polymer called pectin. Pectin is initially synthesized as an esterified molecule in the Golgi and is then selectively deesterified in the cell wall by pectin methyl esterases (PMEs). The most common pectin is homogalacturonaic acid (HA), a repeating polymer of α 1-4 D- galacturonic acid (Jarvis, Briggs, & Knox, 2003; Zamil & Geitmann, 2017). Pectin Methylesterases (PME) de-esterify the pectin molecules by breaking the methyl-ester bond at the C-6 residue of the HA polymer, thus removing the methyl group and leaving a negative charge (Sénéchal, Wattier, Rustérucci, & Pelloux, 2014). The resulting negative charge allows de-esterified pectin to crosslink with Ca^{2+} and form a gel-like network that spans between cell walls and contributes to cell adhesion (Daher & Braybrook, 2015; Steele, McCann, & Roberts, 1997).

The middle lamella is formed during cytokinesis when a cell plate made of pectin is laid down between the two daughter cells (Zamil & Geitmann, 2017). The pectin and other materials

are delivered to the site of cell plate formation by the merging of vesicles containing previously constructed cell wall macromolecules, allowing for the rapid creation of the cell plate, and subsequent rapid division of plant cells (Dhonukshe et al., 2006). This cell plate matures along with daughter cells to eventually become the middle lamella. The pectin is largely methyl esterified in the cell plate, but as the cell plate matures into the middle lamella, PME's de-esterify the pectin and allow it to crosslink with Ca^{2+} (Zamil & Geitmann, 2017). Once the middle lamella has been laid down between cells, the primary cell wall is secreted such that the region adjacent to the plasma membranes of the two cells becomes a mesh of cellulose, hemicellulose, and the original pectin. Thus, the middle lamella spans the region between cells and overlaps with the primary wall in regions close to the membrane. No other polysaccharides are deposited in the cell plate, so it remains a region dominated by pectin.

Primary Cell Wall

Cellulose

Cellulose is extruded by the Cellulose Synthase A (CESA) plasma membrane complex as microfibrils consisting of (1,4)-linked β-D-glucans that interweave in order to form strands that are approximately 4 nm in diameter (Cosgrove, 2005). In angiosperms, a crystalline combination of 24-36 (1,4)-linked β-D-glucan chains form the cellulose microfibrils (Carpita, 2011). The *CESA* genes encode a 6 membered rosette protein complex, where each member of the rosette synthesizes a singular microfibril and these microfibrils are linked together to form cellulose bundles (Carpita, 2011). These are all non-redundant in the complex, so if one member of the rosette fails to incorporate into the membrane, the others will also fail (Carpita, 2011). Different subsets of CESA proteins are involved in the synthesis of either the primary cell wall or the secondary cell wall. *AtCesA1, AtCesA3*, and *AtCesA6* all contribute to primary cell wall

cellulose production while *AtCes4, AtCes7*, and *AtCes8* all contribute to secondary cell wall cellulose production (Carpita, 2011). Cellulose synthases have a very short half-life, so they must be continually produced, assembled into rosettes and transported from the Golgi to the plasma membrane for proper cell wall thickening (Haigler & Brown, 1986; Jacob-Wilk, Kurek, Hogan, & Delmer, 2006). In *A. thaliana*, CESAs can be found in Golgi associated complexes that are transported to the cell wall during thickening (Watanabe et al., 2015).

Hemicellulose

In addition to cellulose, plant cell walls also contain the polysaccharide hemicellulose. The most abundant hemicellulose is xyloglucan which crosslinks cellulose microfibrils to form the rigidity necessary for proper turgor pressure and load bearing resistance in plant tissues (Park & Cosgrove, 2015; Perrin et al., 2003). Similarities between the (1→4) β-linked xylopyranosyl linkages in Xylan and the (1→4) β-glycosyl linkages in cellulose provide specific binding between cellulose and xyloglucan to allow them to crosslink (Hayashi, 1989)

Pectin

Pectins make up a collection of polysaccharides rich in galacturonic acid (GalA) and include homogalacturonan (HGA), rhamnogalacturonan-I (RG-I), and rhamnogalacturonan-II (RG-II) (Willats, McCartney, Mackie, & Knox, 2001). These 3 different polysaccharides interweave and covalently link in order to form the pectin network that is present throughout the primary and secondary plant cell wall and dominates in the middle lamella. HGA is a linear polymer formed in the Golgi made up of (1→4))-α-linked-D-galacturonic acid (Liberman et al., 1999; Thibault, Renard, Axelos, Roger, & Crépeau, 1993). The GalA residues on HG pectin are highly methyl esterified, with upwards of 75% of the residues containing a methyl ester group (Goubet & Mohnen, 1999). Further, RG-I is constructed of (1→2)-α-L-rhamnose-(1→4)-α-D-

galacturonic acid repeats (Willats et al., 2001). Finally, RG-II has a 9 (1→4))-α-linked-D-galacturonic acid backbone with 4 different side chains (O'Neill et al., 1996). The levels of each of these pectins varies widely between tissues and species, but the most common is HG pectin.

Through both the addition and cleavage of different functional groups, pectin is changed to alter its flexibility in the gel-like matrix in order for plant cells to expand, or to otherwise respond to pathogens or environmental stress (Wolf, Mouille, & Pelloux, 2009). Pectin Methyl Esterases alter this flexibility by removing methyl groups on pectin and leaving a negative charge. This negative charge allows the pectin to crosslink with Ca^{2+} and form a stiff gel network (Daher & Braybrook, 2015; Steele et al., 1997).

Additionally, some proteins act in opposition to the PME and are known as the Pectin Methylesterase Inhibitors (PMEI). PMEIs work by covering the pectin binding site on PMEs, thus preventing them from de-esterifying the pectin (Hothorn, Wolf, Aloy, Greiner, & Scheffzek, 2004; Wormit & Usadel, 2018). A single PMEI can bind to and affect multiple PMEs, and their activity has been linked to an increase in resistance to pathogen infection (Liu et al., 2018).

De-esterified pectin is the target of cleavage by polygalacturonases (PGs). These enzymes are involved in the process of cell separation, such that plant tissues can expand and grow (Xiao, Somerville, & Anderson, 2014). PGs hydrolyze pectin, thus loosening the cell wall and allowing for cell separation, growth, and expansion. However, since they only target de-esterified pectin, PG activity is dependent on PME activity. Since PME activity increases cellular adhesion by increasing calcium cross-linking and PG activity decreases adhesion, the balance between the activity them will determine the relative amounts of adhesion. Consequently, in some tissues like root border cells, an increase in pectin methyl esterification is linked to an

increase in cellular cell separation, while in the mesophyll it is linked to an increase in cellular adhesion (Lionetti, Cervone, & De Lorenzo, 2015; Wen, Zhu, & Hawes, 1999).

Cell Wall Proteins

A class of proteins called plant cell wall associated kinases (WAKs) act as pectin receptors in plants (Kohorn & Kohorn, 2012). These proteins have a threonine/serine cytoplasmic kinase domain, as well as an extracellular domain comprised of multiple epidermal growth factor repeats (He, Cheeseman, He, & Kohorn, 1999). WAKs bind to negatively charged deesterified pectin via the positively charged residues in the extracellular domain (Decreux et al., 2006). WAKs initially colocalize with pectin in the Golgi, and are then transported to the plasma membrane by Golgi vesicles (Kohorn et al., 2006). They bind not only to native long polymers of pectin in the wall, but also to pectin fragments, or oligogalacturonides (OGs) which are generated by pathogens and wounding (Kohorn et al., 2009). WAKs are thought to be required for the regulation of the cell wall during development, but also a response to pathogen. In both scenarios WAKs act as a regulatory pectin sensor for plants (Kohorn, 2015).

Extensins and arabinogalactan proteins (AGPs) are a family of hydroxyproline-rich glycoproteins (HRGPS) in the primary cell wall (Herger, Dünser, Kleine-Vehn, & Ringli, 2019). Extensins have a rod like structure characterized by variations of repeating Ser-Hyp-Hyp-Hyp-Hyp(SO_4), and can bind to one another utilizing tyrosine residues in order to form extensin networks in the plant cell wall (Fry, 1982; Showalter & Basu, 2016). This network is critical to the growth of the plant cell, as well as its response to environmental changes and defense against pathogen invasion. In *A. thaliana,* a mutant extensin AtEXT3 does not allow for proper cross wall assembly and leads to developmental defects (Cannon et al., 2008). AGPs are more heavily

glycosylated than extensins and are characterized by their dipeptide motifs including Ser-Pro, Ala-Pro, Thr-Pro and Val-Pro. Their structural make up is a core protein, with surrounding arabinose and galactose rich side chains (Seifert & Roberts, 2007; Showalter & Basu, 2016). These proteins are anchored in the plasma membrane via a Glycosylphosphatidylinositol (GPI) anchor and have been implicated in the processes of cell division, and inhibitory signaling during embryogenesis (Seifert & Roberts, 2007; Showalter & Basu, 2016).

Cellular Adhesion

Given that the middle lamella lies at the junction of plant cell walls, it plays an important role in the interactions between cells and cellular adhesion. (Zamil & Geitmann, 2017). Adhesion likely occurs through Ca^{2+} crosslinking of de-esterified HG pectin in the middle lamella. When grown with one-tenth the amount of calcium, rather than forming a typical lattice pattern of pectin in newly formed cell wall, plants form dense aggregations of pectin (Domozych et al., 2014). These dense aggregations are not able to bind plant cells to one another like the typical lattice structure, showing that calcium and calcium cross-linking is critical to cellular adhesion. Additionally, treatments with various calcium chelators result in cell separation, supporting the notion that Ca^{2+} crosslinking constructs a pectin network that results in cellular adhesion (Domozych et al., 2014). In order to bind neighboring cells together, it is likely that the Ca^{2+} cross linking of deesterified pectin links together the pectin present in the middle lamella to the pectin present in the primary cell wall.

Adhesion mutants

Genetic analyses of adhesion in *A. thaliana* have revealed the importance of pectin and several proteins involved in cellular adhesion. *QUASIMODO2* (*QUA2)* encodes a Golgi

localized protein with a critical methyltransferase domain (Mouille et al., 2007). Plants homozygous for a mutant *qua2* allele demonstrate decreased growth, as well as reduced cell adhesion and a 50% reduction in HG pectin content in the cell wall. In addition, *qua2* mutants have irregularly detached epidermal cells in their hypocotyls (Mouille et al., 2007). However, while the overall level of pectin content in *qua2* mutants is reduced, there is no significant change in the degree of methylesterification, leading to the conclusion that *QUA2* is not responsible for the pectin methylesterification on its own (Du et al., 2020). This analysis of *QUA2* demonstrates that pectin abundance helps determine the level to which plant cells adhere to one another. However, not all adhesion mutants have changes to their pectin abundance. To that end, another Golgi localized protein *FRIABLE1 (FRB1)* is critical to cell adhesion in *A. thaliana*, and when mutated, produces cell-adhesion deficient mutants. In this case however, the mutant phenotype is thought to come from a change in the relative abundances of both galactose and arabinose in the plants (Neumetzler et al., 2012). In *frb1* mutants, arabinose content is increased by up to 80%, and galactose was reduced by 7%. Additionally, there are a number of genes that experience upregulation in *frb1* mutants including PMEIs. Taken together, *FRB1* and *QUA2* indicate that pectin abundance in addition to pectin modifications are important for cellular adhesion (Mouille et al., 2007; Neumetzler et al., 2012).

A genetic suppressor analysis also identified additional regulatory pathways in adhesion. *Esmeralda1 (ESMD1)* encodes a putative Golgi-localized *O-fucosyltransferase,* and the *esmd1* mutant can restore the *qua2* adhesion deficiency (Verger, Chabout, Gineau, & Mouille, 2016). Although *esmd1* does not restore pectin levels, it is still able to rescue *qua2-1/esmd1-1* and *qua2-1/frb1-2/esmd1-1* mutants and prevent a mutant phenotype, suggesting that *esmd1* restores cellular adhesion through the repression of a pectin-related signal pathway. This suggests that the

regulation of cellular adhesion is not solely driven by pectin content and modification. There is a possibility that WAKs, since they have multiple EGFR repeats thought to be the substrate of fucosyl transferases, are being fucosylated by ESMD1 as a part in a pectin perception pathway (Kohorn, Greed, Verger, Mouille, & Kohorn, 2021).

To identify additional mutations that affect cell adhesion, the Kohorn Laboratory performed a screen of mutagenized Arabidopsis seedlings. Numerous mutants were isolated and one mutant is called *ELMO1* and encodes a novel Golgi protein that has no enzymatic domains (Kohorn, Zorensky, et al., 2021). *elmo1* results in reduced cellular adhesion and a 2.6 fold reduction in mannose levels, while pectin content and methyl esterification, cellulose, and hemicellulose are unaffected (Kohorn, Zorensky, et al., 2021). The mutant adhesion phenotype produced by *elmo1*, however, is relatively weak when compared to *qua2* and *frb1* mutants. Similar to *frb1 and qua2*, *elmo1* is suppressed by *esmd1* suggesting that *ELMO1* is involved in a cellular adhesion signaling pathway. It is possible that *ELMO1* is involved in a mannose dependent quality control mechanism for Golgi processed cell wall proteins. However, it is also possible that *ELMO1* regulates pectin abundance and pectin changes were not detected since it is a weak allele (Kohorn, Zorensky, et al., 2021). There are 5 other *ELMO*-like genes in the Arabidopsis genome that encode Golgi proteins of similar size and structure, and these homologues may provide redundancy. This redundancy likely explains the relatively weak phenotype of *elmo1* compared to other cellular adhesion mutants.

My bioinformatic analysis identified ELMO1 homologues in many vascular plants, and five ELMO homologues in Arabidopsis. This project will focus on *ELMO1* and *ELMO2* which have 79% amino acid similarity. Molecular modeling of *ELMO1* suggests a coil-coil structure, and given the high amino acid similarity, it is likely that *ELMO2* has this same structure.

Mutations in *ELMO1* provide a weak adhesion phenotype, while *elmo2* mutants appear wild type. However, *elmo1,2* double mutants have greatly reduced cellular adhesion indicating that *ELMO1* and *ELMO2* are redundant.

Methods

DNA Extraction

1-2 leaves from soil grown plants were frozen in liquid nitrogen and stored in -80°C. Leaves were then homogenized with a plastic drill bit in an Eppendorf tube using 400 µl DNA extraction buffer (1 M Tris pH 7.5 to 8, 5 M NaCl, 0.5 M EDTA, 10% SDS) before being incubated at 55°C for 10 minutes. The sample was then vortexed briefly and centrifuged for 5 minutes at 20,000 x g. 350 µl supernatant was removed and mixed with an equal volume of isopropanol and incubated for 10 minutes at room temperature. Samples were centrifuged at 20,000 x g, and the supernatant was discarded. DNA pellet was then rinsed with 70% ethanol and centrifuged at 20,000 x g for 1 minute, discarding the supernatant after spin. The pellet was centrifuged again at 20,000 x g for 15 seconds to remove excess ethanol. Pellets were left to air dry for 30 minutes before being suspended in 100 µl H_2O. DNA was stored at -20°C.

Titanium-TAQ PCR

PCR reaction: For a 25 µl reaction, the PCR master mix contained 17 µl dH_2O, 5 µl 10X Titanium buffer, 0.5 µl of 2.5 mM dNTPs, 0.5 µl of 10 µM forward primer, 0.5 µl of 10 µM reverse primer, 0.5 µl Titanium Taq polymerase, and 1 µl *A. thaliana* DNA template. Reaction parameters were as follows: 1 minute 98°C, then 30 cycles of 30 seconds at 98°C for denaturation, 30 seconds at 58°C for annealing, and 1 minute at 72°C for extension. After all 30 cycles were completed, the reaction as held for 2 minutes at 72°C and stored at 4°C.

Table 1.PCR Primers

Product:	Forward Primer:	Reverse Primer:
WT *ELMO2:* 360bp	At1g05070F: GCAAAGCACGATCCAGAGGTGAAC	At1g05070R: CTCACCTAAGAAACTGTGATTGCTTAA TCCTGC
tDNA *ELMO2:* 259bp	At1g05070F: GCAAAGCACGATCCAGAGGTGAAC	LBb1.3: ATTTTGCCGATTTCGGAAC
ELMO1: 650bp	Elmo1seqF: GACTCAGCAATGGTTCATTCACTG	Elmo1seqR: CCTCAGTGCCGCTTTTGGATTTAACAG

Ruthenium Red Staining

Seeds were sterilized using 95% ethanol and 10% bleach before being washed twice with sterile water and put in 5ml liquid MS media. These seeds were then placed in the cold for 48 hours and subsequently subjected to four hours of light before being grown in the dark for four days. After four days, the seedlings were stained with 2ml of 0.5 mg/ml of ruthenium red dye for two minutes before being washed twice with dH_2O. The stained seedlings were then visualized with a Leica dissecting microscope to determine any defective cellular adhesion phenotypes.

Propidium Iodide Staining and Confocal Microscopy

Seedlings were sterilized and grown in the dark according to the same protocol for ruthenium red staining. After growing in the dark for 4-days, the seedlings were stained with 10 µg/mL propidium iodide before being washed one time with dH_2O. Stained seedlings were visualized with a Leica SP8 confocal microscope using a 514nm excitation laser and detection at 520-560 nm.

Measuring Length of Roots and Hypocotyls

ImageJ was used to measure the lengths of the roots and hypocotyls of seedlings. Relative lengths were converted to physical lengths using a standard pixel value of 1cm=1152 pixels at 10x magnification. Statistical analysis was performed in R. One-way ANOVAs were performed on hypocotyl length and root length for seedlings of each mutation. Following these ANOVAs, Tukey's HSD test was run in each case.

Results

ELMO1 encodes a Golgi protein involved in cell adhesion in Arabidopsis (Kohorn, Zorensky, et al., 2021). *ELMO1* mutants appear to have reduced mannose content in the cell wall, but since it is a weak allele, it remains possible that a slightly reduced pectin content may not have been detected (Kohorn, Zorensky, et al., 2021). A bioinformatics-based investigation was performed on the *ELMO1* gene in order to determine its conservation across the plant kingdom. First, using The Arabidopsis Information Resource (TAIR) database, the protein sequence encoded by *ELMO1* (AT2G32580) was predicted. Then, using BLASTp, 29 sequence matches were found within the plant kingdom. These matches were found in species ranging across crop plants including *Malus domestica, Oryza sativa, Zea mays, Vigna radiata,* as well as many other plant species. These sequences were aligned using Clustal-Omega's multiple sequence alignment tool and visualized in Jalview 2.11.1.3. and the results are shown in Figure 1, where blue highlights similar or identical amino acids.

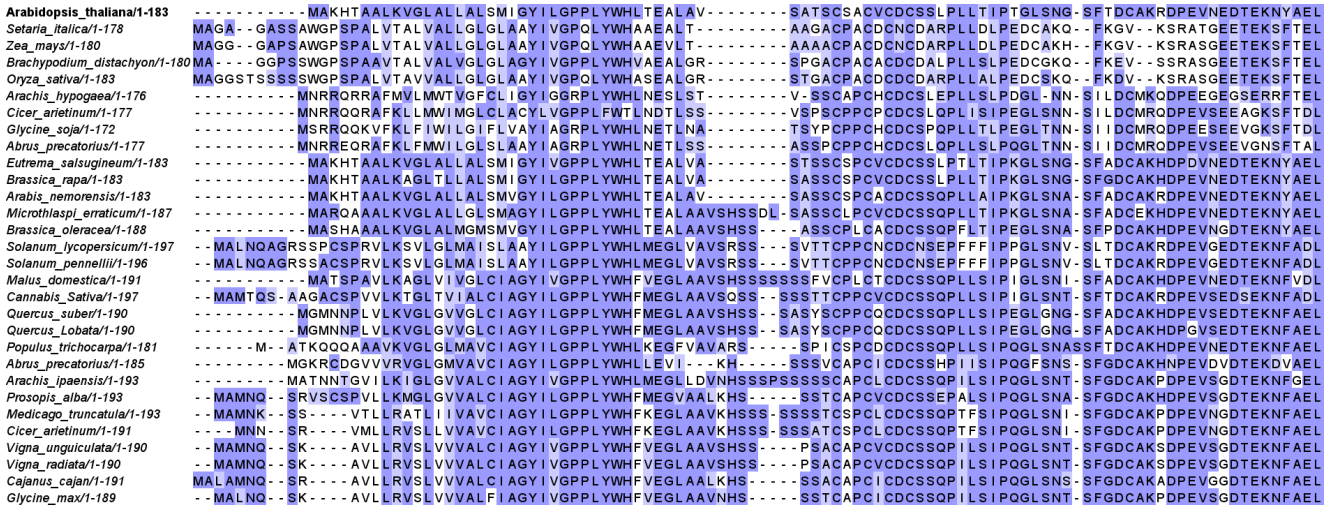

Figure 1. ELMO1 Amino Acid Sequence Alignment across species. All sequences were compared to the *Arabidopsis thaliana* sequence for ELMO1, bolded and shown on the top line. Darker shades of blue indicate increasing sequence similarity with reference to the *Arabidopsis thaliana* sequence. Dashes indicate missing amino acids.

Two distinct variations were found within the ELMO sequences. Firstly, surrounding amino acid 39, in many cases there was an 8-9 amino acid deletion and in some cases this deletion was only partial. Additionally, at amino acid 70, there was another variation featuring a double amino acid deletion resulting in the sequence: V--KSRA. Noting these mutations, a cladogram was constructed of all species that produced matches along with their mutations and whether the species was a monocot or dicot. This cladogram is shown in Figure 2. Plants that had both the amino acid 39 and 70 variations were monocots in all cases, while those that had just the position 39 variation were dicots. Additionally, no plants that had the 70-position mutation were without the mutation at amino acid 39. At present, it is not known if this position 39 and 70 variation only occurs on monocots, as the sample size relative to the plant kingdom is small.

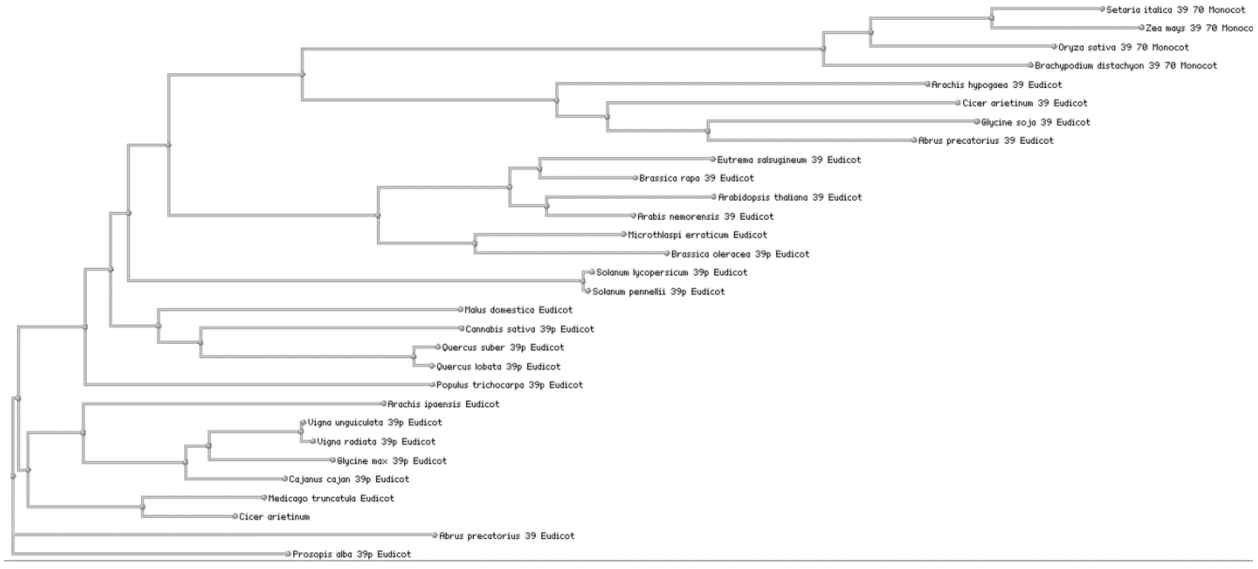

Figure 2. Cladogram of ELMO1 Variations. Length of lines between nodes is proportional to evolutionary distance between nodes. Numbers next to species name indicate which variation was identified in the sequence where 39p indicates a partial deletion at amino acid 39 relative to the others.

Following the identification of these variations in vascular plants, approximate structural models of proteins containing these different variations were generated using the Swiss tool

EXPASY (Bertoni, Kiefer, Biasini, Bordoli, & Schwede, 2017; Bienert et al., 2017; Guex, Peitsch, & Schwede, 2009; Studer et al., 2020; Waterhouse et al., 2018). This tool uses known protein structures and a given amino acid sequence in order to give an approximation of the unknown structure. Sequences from *Malus domestica, Arabidopsis thaliana,* and *Zea ma*ys were chosen as representative of the different sequence types observed. In each case, the predicted model showed a coil-coil protein structure as indicated in Figure 3. In all cases the variation at amino acid 39 or 70 variation will be in the longer coil of the protein. These estimated models show that neither the amino acid 39 nor the amino acid 70 variation on the ELMO1 protein likely change the coil-coil protein structure. Thus, these variations could be an insignificant consequence of speciation. Additionally, it is possible that these variations are consistent across all of the *ELMO*-like genes, or they may differ depending on the homologue. However, given that these models are estimations, the variations could have an effect on structure or function of the ELMO1 protein, and more detailed protein modeling is needed to determine this.

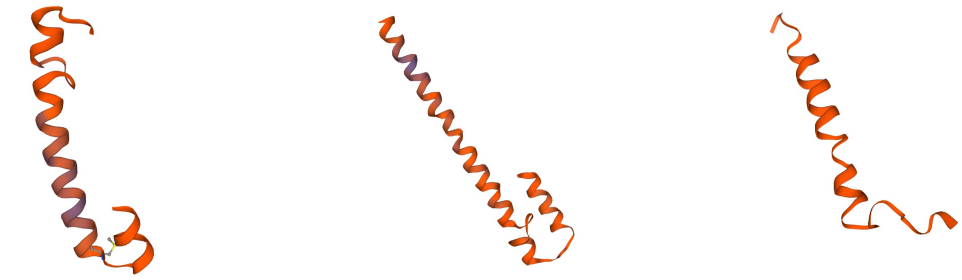

Figure 3. Potential Protein Structure of ELMO1. Protein structures of ELMO1 as estimated by EXPASY for each potential variation where number beside organism name indicates variation. In each case the protein is predicted to have a coil-coil structure, with potential variations being on the longer coil.

Five homologues of ELMO1 in *Arabidopsis thaliana* were identified by using various databases including Uniprot and TAIR, and their sequences are shown in Figure 4, where the darker blue indicates identical amino acid sequence, while light blue shows similar amino acids to ELMO1. Database searches using SUBA have shown that all proteins are predicted to localize to the Golgi and appear to have similar predicted protein structures. The consequence of the variations in these sequences are not known. At3g24290 is identical to At4g30996 except for a 24 bp insertion and is listed only in the NIH sequencing database and not annotated as a gene in the Arabidopsis data base. Therefore, it likely represents a splice variant or a sequencing error. Due to the high sequence similarity between them, the family members were assigned ELMO names as following; *ELMO1* At2g32580; *ELMO2* At1g05070; *ELMO3* At4g04360; *ELMO4* At4g30996, *ELMO5* At2g24290 (Kohorn, Zorensky, et al., 2021).

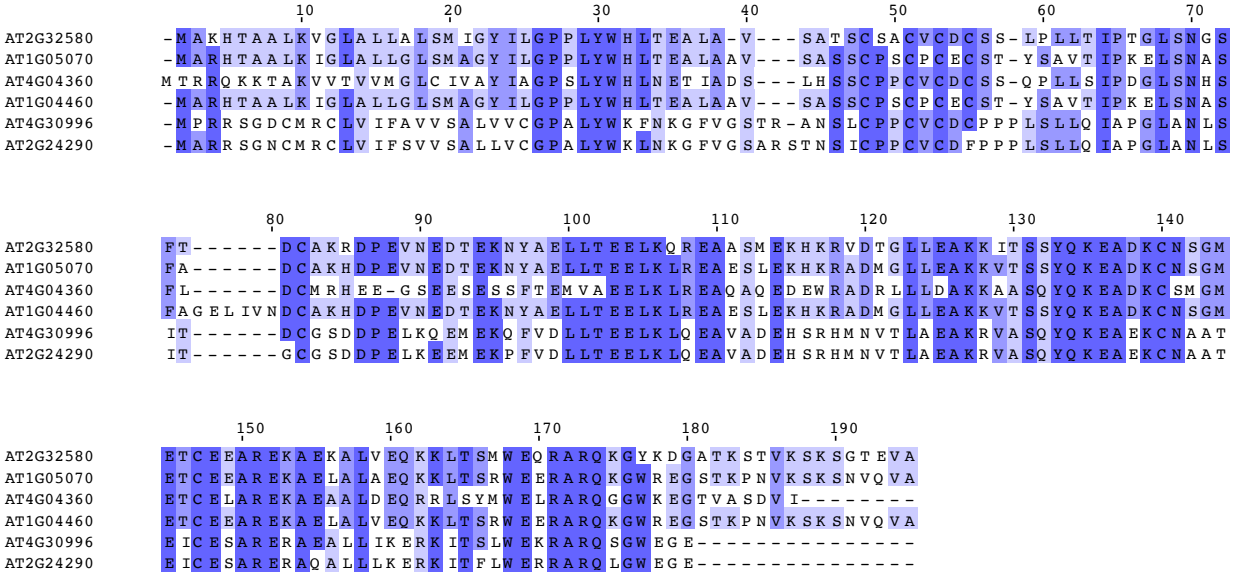

Figure 4. Sequence Alignment of all ELMO-like genes in *Arabidopsis thaliana*. Darker shades of blue indicate higher sequence similarity and dashes indicate missing amino acids.

Identification of T-DNA Mutants

To determine if the *ELMO* homologues are involved in cellular adhesion, mutant alleles of the genes were identified, and this thesis focused on *ELMO1* and *ELMO2*. Seeds having a T-DNA insertion in At1g05070 (*ELMO2*) were ordered from the Arabidopsis stock center (Kohorn, Zorensky, et al., 2021). To detect the presence of the T-DNA insertion in these plant lines, primers were made where one primer base paired at one end of the T-DNA (green arrow Figure 5) and the other in the flanking *A. thaliana* DNA (Red arrow Figure 5). Primers that flanked the T-DNA insertion site were used to identify wild type alleles, but since the T-DNA is so large, genes containing the T-DNA insertion would not amplify under the PCR conditions used. These two sets of primers were used in PCR reactions to amplify sample DNA from plants potentially containing a T-DNA insertion in *ELMO2.* Successful amplification of the T-DNA insertion should produce a 259bp product. Figure 5 shows that this product was detected in *elmo2* mutant plants but not in wild type, thus confirming that the insertion is present. Since not all plants had the insertion, the parental line was assumed to be heterozygous for the insertion. The PCR product was sequenced to confirm the insertion site. Additionally, primers that flank the T-DNA insertion region successfully produced a product for each plant tested, confirming that the plants were heterozygous for the insertion (PCR performed by Bruce due to Covid-19 shutdown, data not shown). One heterozygous plant was self-crossed, and the F1 were then screened for a plant homozygous for the T-DNA insertion.

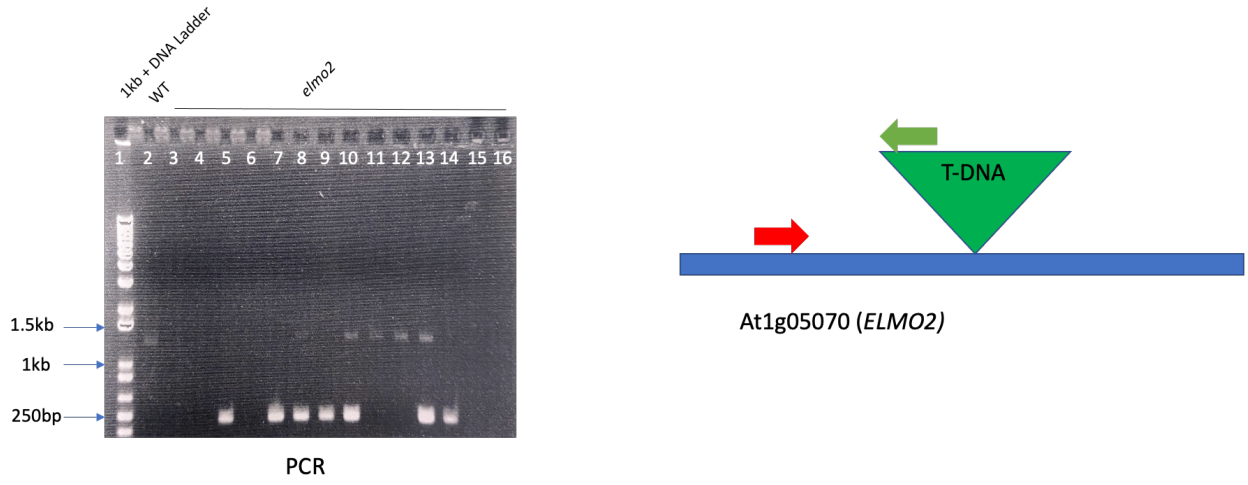

Figure 5. ELMO2 T-DNA PCR. Lane 1: 1kb+ DNA Lane 2: WT Control DNA. Lane 3-16: elmo2 T-DNA DNA samples. Bands in lanes 5,7-10,13,14 indicate that the T-DNA insertion was successful in those plants. Graphic to the right shows both the T-DNA insertion into the genome, and the primers used to detect it. 1.2 kb band present in lanes 2, 8, 10-13 are a nonspecific product. The expected T-DNA product is the 250bp product in lanes 5,7-10,13,14.

Upon identification of an *elmo2* homozygote, it was crossed to an *elmo1* homozygote. Using the above methods, PCR reactions were performed for amplification of WT *ELMO1* and *ELMO2*, and mutant *elmo1* and *elmo2*. The F1 generation of this cross was screened for plants heterozygous for both mutations. Upon identification, heterozygotes were self-crossed and the resulting F2 population was screened for a plant homozygous for both *elmo1* and *elmo2*.

Mutant Phenotypes

Ruthenium Red dye will stain the roots but not the hypocotyls of WT dark-grown seedlings and will stain the hypocotyls in cellular adhesion mutants. The ability to stain hypocotyls in adhesion mutants likely comes from increased penetration of the cell wall as a result of decreased cellular adhesion. Ruthenium red staining was used in order to determine mutant cellular adhesion phenotypes in *elmo1*$^{-/-}$, *elmo2* $^{-/-}$ and *elmo1*$^{-/-}$*elmo2*$^{-/-}$ plants. *elmo1*$^{-/-}$ mutants show the expected red staining (Figure 6A). *elmo2*$^{-/-}$ mutants on their own did not stain

red and had no mutant adhesion phenotype (Figure 6A). However, *elmo1*$^{-/-}$*elmo2*$^{-/-}$ double mutants produced a strong mutant phenotype including curling disrupted hypocotyl cells and strong red staining. Propidium iodide was used as a general surface stain and stained hypocotyls were visualized using confocal microscopy and 3D reconstruction. As expected, *elmo1*$^{-/-}$ shows occasional cells curling away from the hypocotyl where they otherwise do not in WT (Figure 6B). *elmo2*$^{-/-}$ shows no difference from WT (Figure 6B). *elmo1*$^{-/}$ *elmo2*$^{-/-}$ mutants have disorganized cells peeling away from the overall tissue structure (Figure 6B).

The root and hypocotyl length of each mutant was also measured. *elmo1*$^{-/-}$ *elmo2*$^{-/-}$ mutants have both significantly smaller root and hypocotyl lengths compared to WT (Figure 7). Additionally, *elmo1*$^{-/-}$ mutants have a significantly smaller hypocotyl compared to WT. Taken together, these data suggest that *elmo2* is partially redundant to *elmo1*.

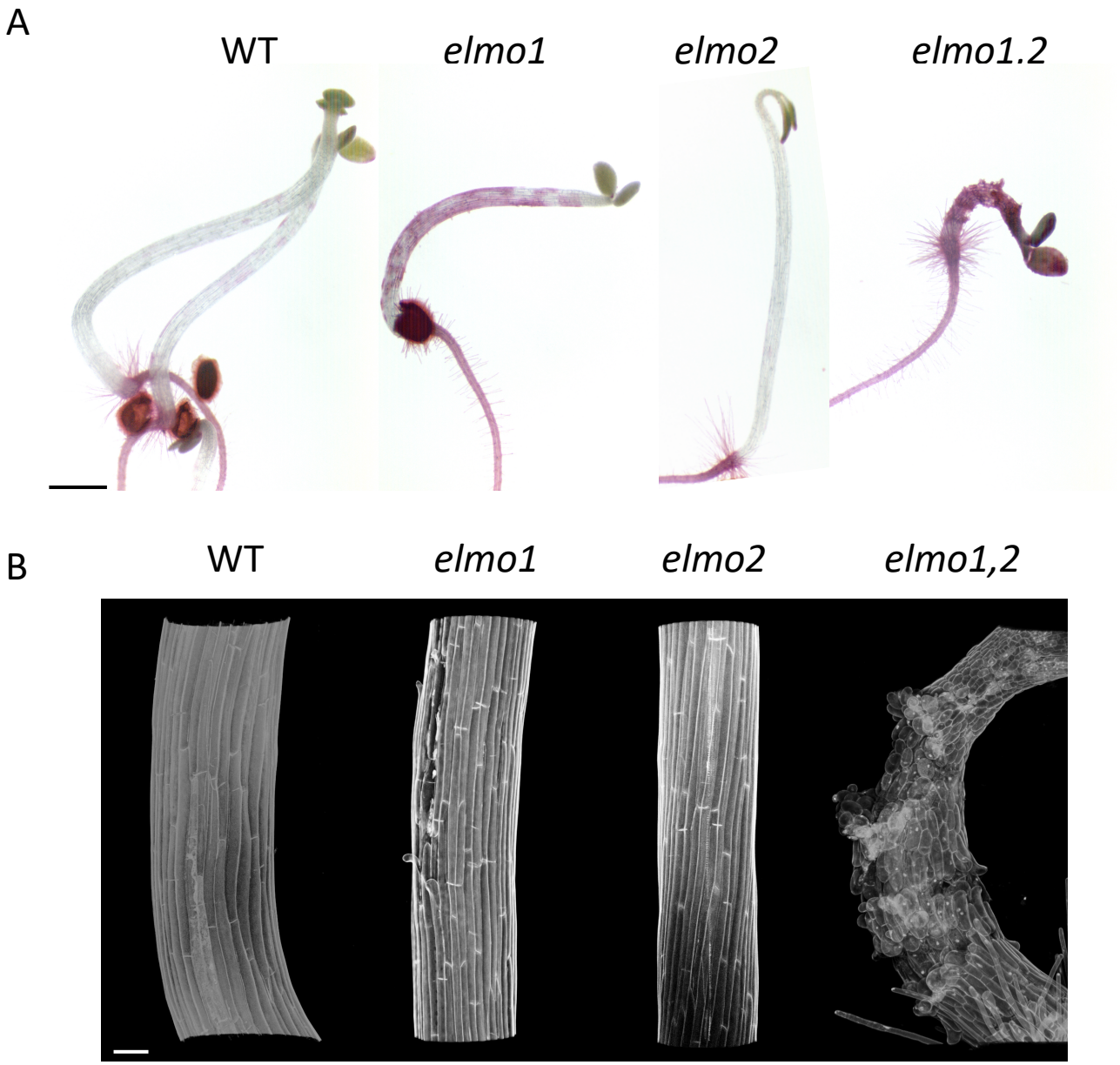

Figure 6. Seedlings with mutant ELMO-Like genes. A. Dark-grown seedlings after being subjected to ruthenium red staining. B. Confocal microscopy of dark-grown propidium iodide-stained seedling hypocotyls. elmo1 and elmo1,2 demonstrate defective cellular adhesion phenotypes, while WT and elmo2. Bar indicates 1mm in A and 100µm in B.

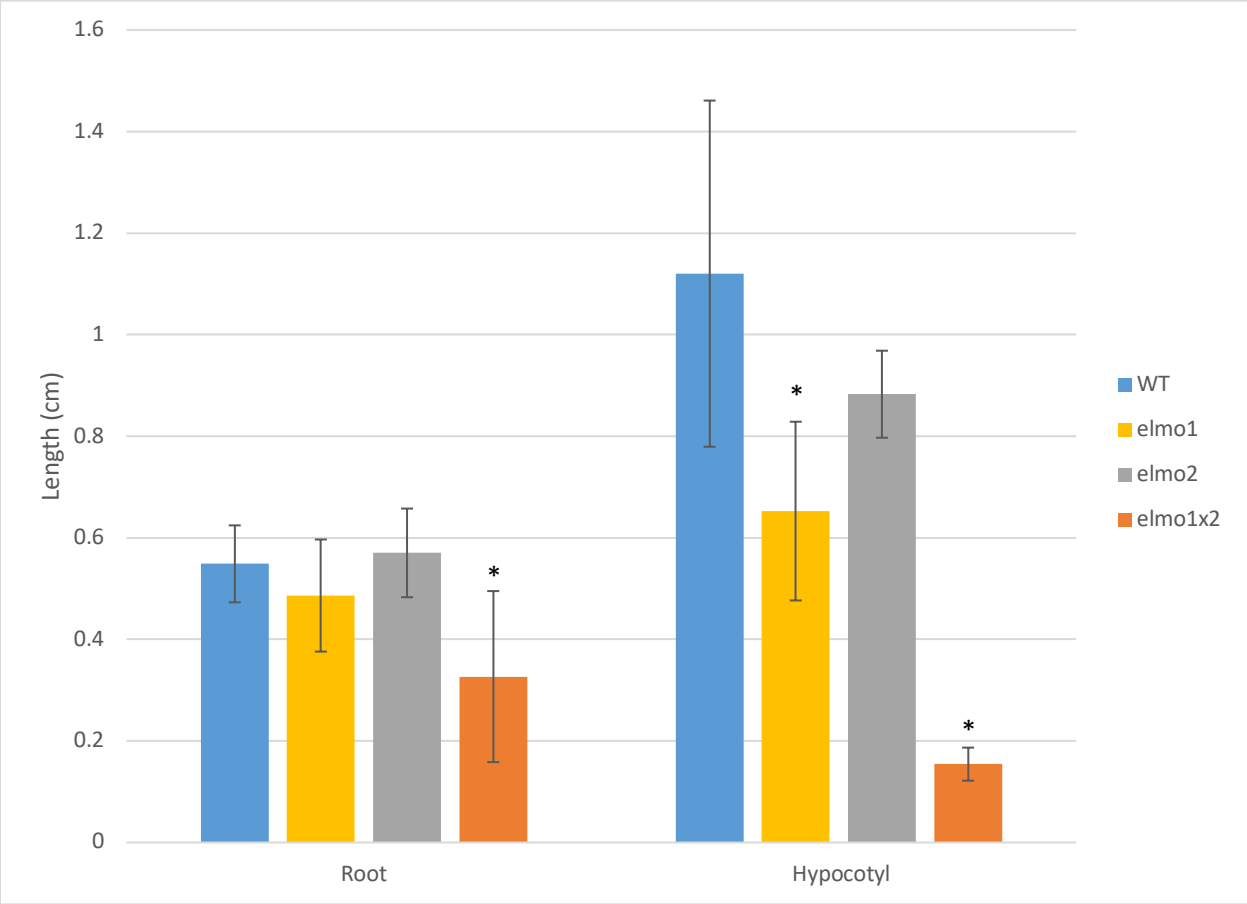

Figure 7. Root and Hypocotyl Lengths of ELMO-like mutants. *elmo1/2* was significantly smaller in all cases compared to WT (p-values: 0.011, <0.001, for Root and Hypocotyl lengths respectively. *elmo1* had significantly smaller hypocotyl and total length than WT (p-value: 0.002 & 0.004 respectively). Asterisks indicate p-values< 0.05 compared to WT. Single-way ANOVA and Tukey's HSD test were performed in R.

Discussion

The plant cell wall is a matrix of polysaccharides laid down on the exterior of the plasma membrane. This matrix includes layers of cellulose, hemicellulose and pectin along with numerous proteins (Keegstra, 2010). The middle lamella, a region dominated by pectin between plant cell walls, is thought to be responsible for cellular adhesion between neighboring plant cells (Zamil & Geitmann, 2017). EMS mutagenesis of Arabidopsis seeds revealed a plant with mutant cellular adhesion named *elmo1* that exhibits patchy staining of Ruthenium Red on the hypocotyls, cell curling and sloughing of cells on the hypocotyl and reduced mannose content (Kohorn, Zorensky, et al., 2021). *ELMO1* encodes a 20kDa non-enzymatic Golgi protein with homologues in vascular plants and a family of 5 ELMOs in the *Arabidopsis thaliana* genome.

To determine if members of the *ELMO* family of proteins are redundant, an *elmo2* mutant was identified with a T-DNA insertion in the coding region of the gene. After isolating a plant homozygous for the *elmo2* mutant allele, it was crossed to an *elmo1* mutant and the progeny screened to find an $elmo1^{-/-}elmo2^{-/-}$ double mutant. $elmo1^{-/-}$, $elmo2^{-/-}$ and $elmo1^{-/-}elmo2^{-/-}$ seedlings were stained with Ruthenium Red in order to determine mutant cellular adhesion phenotypes. Ruthenium red staining confirms the previously identified mutant adhesion phenotype of *elmo1*. As evident in Figure 6, $elmo1^{-/-}$ mutants demonstrate patchy Ruthenium Red staining in the hypocotyl as well as gapping of hypocotyl cells shown by confocal microscopy of propidium iodide-stained seedlings. Ruthenium red staining of $elmo2^{-/-}$ revealed that there is no defective cellular adhesion phenotype for $elmo2^{-/-}$ mutants (Figure 6A). This lack of a phenotype was confirmed by confocal microscopy of propidium iodide-stained seedlings, and a lack of changes to root or hypocotyl length compared to WT (Figure 6B & Figure 7). The combination of both an

elmo1$^{-/-}$ and *elmo2*$^{-/-}$ mutation, however, produces a dramatic mutant phenotype characterized by significantly smaller roots and hypocotyls compared to WT, and significantly smaller hypocotyls compared to *elmo1* (Figure 7). Further, confocal microscopy of propidium iodide staining seedlings shows far more disorganization and large gaps between cells in the hypocotyl tissue in *elmo1*$^{-/-}$*elmo2*$^{-/-}$ mutants compared to *elmo1*$^{-/-}$ (Figure 6B)

While the *elmo2*$^{-/-}$ mutants do not display a mutant adhesion phenotype, the *elmo1*$^{-/-}$ *elmo2*$^{-/-}$ mutants do. The gapping in *elmo1*$^{-/-}$*elmo2*$^{-/-}$mutants is similar to that of *qua2*-1 and *frb1-2* and the reduction in hypocotyl length is in accordance with previous observations of cellular adhesion mutants (Verger et al., 2016). The phenotype displayed by *elmo1*$^{-/-}$*elmo2*$^{-/-}$ is also similar to that of *elmo1*$^{-/-}$ but more severe (Kohorn, Zorensky, et al., 2021). Given that *elmo2*$^{-/-}$ shows no phenotype on its own, the increase in severity of this phenotype indicates that ELMO2 serves as a partially redundant protein to ELMO1.

Alterations to pectin levels, pectin modifications, or pectin related signaling usually leads to defects in adhesion (Mouille et al., 2007; Neumetzler et al., 2012; Verger et al., 2016). In a cell wall analysis of *qua*2 mutants, a 50% reduction in pectin content was found, and large changes in the modification of pectin were found in *friable1* mutants. In initial cell wall analyses of *elmo1* mutants performed in Brunswick, measurements of galacturonic acid levels were lower relative to WT. However, our collaborators in Versailles were unable to detect this difference and it is likely that a small difference in the assay between Brunswick and Versailles accounts for the discrepancy. However, since the whole cell wall analysis that included cellulose and neutral sugars was performed in Versailles, only the complete data set could be published. Analysis of highly similar *qua* mutant alleles indeed reveal discrepancies between changes in pectin levels depending on which lab is performing the assay (Gao, Xin, & Zheng, 2008; Mouille

et al., 2007). Despite high amino acid similarity with *qua2-1*, *qua3* mutants do not demonstrate a mutant cellular adhesion phenotype, indicating redundancy between proteins involved in cellular adhesion. Redundancy within similar proteins is also detected in the ELMO family. *elmo1*$^{-/-}$ *elmo2*$^{-/-}$ double mutants produce a stronger phenotype than *elmo1*$^{-/-}$ and *elmo2*$^{-/-}$ mutants, the latter having no phenotype at all. It is expected that the *elmo1*$^{-/-}$*elmo2*$^{-/-}$ will have a reduced pectin content, a deficiency significant enough to be detected by the assay.

A difference in mannose levels was detected in the *elmo1* mutants. Compared to WT, *elmo1*$^{-/-}$ has a 2.6 fold reduction in mannose content as indicated by total cell wall analysis, with no change in galacturonic acid levels between the two (Kohorn, Zorensky, et al., 2021). *elmo2*$^{-/-}$ and *elmo1*$^{-/-}$ *elmo2*$^{-/-}$ mutants are expected to share this drop in mannose. This *elmo1* induced mannose reduction may be affecting the GPI anchor on AGPs involved in cellular adhesion, as mannose is a critical component in these anchors (Kohorn, Zorensky, et al., 2021). However, the ELMO family of proteins may also be involved in a mannose-based quality control mechanism for proteins originating in the Golgi. ELMO1 is predicted to be a scaffold for proteins involved in this process since no enzymatic domains can be identified in the protein (Kohorn, Zorensky, et al., 2021). Non-enzymatic scaffold proteins are facilitators of signal transduction and enzymatic pathways by linking proteins together in a complex. For example, the yeast protein Ste5 forms a complex with other protein kinases in the mitogen-activated protein kinase (MAPK) cascade to facilitate signal transduction required for mating (Chol, Satterberg, Lyons, & Elion, 1994). Ste5 has an active role in the MAPK cascade wherein it phosphorylates one member of the complex Fus3 which reduces pathway output (Bhattacharyya et al., 2006). If ELMO2 is redundant to ELMO1, then we can expect that it is also a scaffold and is involved in the same cell wall

biosynthesis or cellular adhesion signaling pathway and that mutation of both genes will severely damage cellular adhesion.

To further support this idea that ELMO2 is redundant to ELMO1, colocalization assays of ELMO1 and ELMO2 must be performed. Their locations relative to each other will be critical in understanding if their functions are redundant; if they are in different areas of the cell or expressed in different cell types or organs, it is unlikely they are performing the same action. Constructing a GFP-fusion of ELMO1 has revealed that it localizes to the Golgi in *A. thaliana* cells, but its localization with other proteins has not yet been explored (Kohorn, Zorensky, et al., 2021). Colocalization with other proteins critical to cellular adhesion like QUA2 would be helpful at determining whether ELMO1 and ELMO2 are scaffold proteins. Mutation of another ELMO family protein *ELMO4* also leads to a dramatic cellular adhesion phenotype. The Pearson group in Copenhagen found that *elmo4* mutants have reduced pectin, and a similar phenotype to *elmo1,2* mutants (Unpublished Data). This group has also performed a bi-fluorescence assay on QUA1 and ELMO4. This approach takes advantage of two proteins tagged with either the amino terminal or carboxyl terminal half of YFP. If the two proteins bind, then the two halves of YFP are brought together to restore YFP activity. The only way for this bi-fluorescence to occur would be for the two proteins containing the YFP halves to be in extremely close proximity. The Copenhagen group has seen success with this bi-fluorescence assay utilizing ELMO4 and QUA1, providing support that the *ELMO*-like proteins are acting as a scaffold for proteins involved in pectin biosynthesis pathways. The Kohorn lab is performing similar experiments with ELMO1 and ELMO2.

That an ELMO-like protein has been observed to colocalize with a protein known to be critical to pectin biosynthesis supports the notion that ELMO1 and ELMO2 are involved in a

pectin-related cellular adhesion pathway. The ELMO-like proteins show high sequence similarity, so it can be expected that if one of these proteins is associated with a pectin-related protein, they all might serve a similar purpose. To that effect, a suppression assay of *elmo1,2* double mutations with *esmd1* will need to be performed. *esmd1* suppresses mutations in two pectin related cellular adhesion mutations *qua2* and *frb1* (Verger et al., 2016). *elmo1* has also been shown to be suppressed by *esmd1* showing that *elmo1* is involved in a cell wall synthesis or adhesion pathway (Kohorn, Zorensky, et al., 2021). Suppression of *elmo1,2* by *esmd1* will support the notion of their being homologous proteins by demonstrating their involvement in similar if not the same pathways.

Further mutant combinations will need to be performed to fully understand the redundancy of the *ELMO* family. There are 5 known homologues of *ELMO1* in Arabidopsis named *ELMO2, ELMO3, ELMO4, and ELMO5.* The Kohorn Lab has isolated mutants and double mutants of each of these and is exploring their phenotypes. In order to assess further redundancy throughout the *ELMO* family, double mutants of all combinations of *ELMO* family genes will be assessed for mutant phenotypes using Ruthenium Red staining and confocal microscopy of propidium iodide stained seedlings. The presence of a severe mutant phenotype in a double mutant while each single mutant has little to no phenotype will provide evidence of redundancy in each case. Along similar lines, mutants of the *ELMO* family will need to be crossed to known cellular adhesion mutants. Crossing *ELMO*-like mutants to mutants such as *qua2-1* and *frb1,* observing any resulting phenotypes and comparing them to other known phenotypes will paint a broader picture of how different proteins within cellular adhesion pathways interact.

ELMO1 has homologous proteins of high sequence similarities across a variety of species within the plant kingdom (Figure 1). Based on its level of conservation across organisms, I hypothesize that *ELMO1* and subsequently the other *ELMO*-like proteins play a critical role in cellular adhesion across the plant kingdom. Given the diversity of species in which the gene has a homolog, it is likely that this gene has been a part of the genome for a long time. Variations in the amino acid sequence across species did not result in a significant change to the potential protein structure of *ELMO1* (Figure 3). Thus, this protein likely performs the same or similar functions across the plant kingdom.

In conclusion, *elmo2* lacks a mutant cellular adhesion phenotype on its own. When combined with *elmo1*, the resultant *elmo1,2* double mutant produces an additive phenotype far more severe than *elmo1.* This phenotype features significantly shorter hypocotyls in seedlings as well as hypocotyl breakage and gaps between cells. The additive nature of this phenotype supports the proposed notion that *elmo2* is a redundant protein to *elmo1* in *Arabidopsis thaliana.*

References

Bertoni, M., Kiefer, F., Biasini, M., Bordoli, L., & Schwede, T. (2017). Modeling protein quaternary structure of homo-and hetero-oligomers beyond binary interactions by homology. *Scientific Reports, 7*(1), 1-15.

Bhattacharyya, R. P., Reményi, A., Good, M. C., Bashor, C. J., Falick, A. M., & Lim, W. A. (2006). The Ste5 scaffold allosterically modulates signaling output of the yeast mating pathway. *Science, 311*(5762), 822-826. Retrieved from https://science.sciencemag.org/content/sci/311/5762/822.full.pdf

Bienert, S., Waterhouse, A., de Beer, T. A., Tauriello, G., Studer, G., Bordoli, L., & Schwede, T. (2017). The SWISS-MODEL Repository—new features and functionality. *Nucleic Acids Research, 45*(D1), D313-D319. Retrieved from https://www.ncbi.nlm.nih.gov/pmc/articles/PMC5210589/pdf/gkw1132.pdf

Cannon, M. C., Terneus, K., Hall, Q., Tan, L., Wang, Y., Wegenhart, B. L., . . . Kieliszewski, M. J. (2008). Self-assembly of the plant cell wall requires an extensin scaffold. *Proceedings of the National Academy of Sciences, 105*(6), 2226-2231. Retrieved from https://www.ncbi.nlm.nih.gov/pmc/articles/PMC2538902/pdf/zpq2226.pdf

Carpita, N. C. (2011). Update on mechanisms of plant cell wall biosynthesis: how plants make cellulose and other (1→ 4)-β-D-glycans. *Plant Physiology, 155*(1), 171-184. Retrieved from https://www.ncbi.nlm.nih.gov/pmc/articles/PMC3075763/pdf/171.pdf

Chol, K.-Y., Satterberg, B., Lyons, D. M., & Elion, E. A. (1994). Ste5 tethers multiple protein kinases in the MAP kinase cascade required for mating in S. cerevisiae. *Cell, 78*(3), 499-512.

Cosgrove, D. J. (2005). Growth of the plant cell wall. *Nature Reviews Molecular Cell Biology, 6*(11), 850. Retrieved from https://www.nature.com/articles/nrm1746.pdf

Daher, F. B., & Braybrook, S. A. (2015). How to let go: pectin and plant cell adhesion. *Frontiers in Plant Science, 6*(523). doi:10.3389/fpls.2015.00523

Decreux, A., Thomas, A., Spies, B., Brasseur, R., Van Cutsem, P., & Messiaen, J. (2006). In vitro characterization of the homogalacturonan-binding domain of the wall-associated kinase WAK1 using site-directed mutagenesis. *Phytochemistry, 67*(11), 1068-1079.

Dhonukshe, P., Baluška, F., Schlicht, M., Hlavacka, A., Šamaj, J., Friml, J., & Gadella Jr, T. W. (2006). Endocytosis of cell surface material mediates cell plate formation during plant cytokinesis. *Developmental Cell, 10*(1), 137-150.

Domozych, D. S., Sørensen, I., Popper, Z. A., Ochs, J., Andreas, A., Fangel, J. U., . . . Ruisi-Besares, P. (2014). Pectin metabolism and assembly in the cell wall of the charophyte green alga Penium margaritaceum. *Plant Physiology, 165*(1), 105-118. Retrieved from http://www.plantphysiol.org/content/plantphysiol/165/1/105.full.pdf

Du, J., Kirui, A., Huang, S., Wang, L., Barnes, W. J., Kiemle, S. N., . . . Xiao, C. (2020). Mutations in the Pectin Methyltransferase QUASIMODO2 Influence Cellulose Biosynthesis and Wall Integrity in Arabidopsis. *The Plant Cell, 32*(11), 3576-3597. doi:10.1105/tpc.20.00252

Fry, S. (1982). Isodityrosine, a new cross-linking amino acid from plant cell-wall glycoprotein. *The Biochemical Journal, 204*(2), 449-455.

Gao, P., Xin, Z., & Zheng, Z.-L. (2008). The OSU1/QUA2/TSD2-encoded putative methyltransferase is a critical modulator of carbon and nitrogen nutrient balance response in Arabidopsis. *PLoS One, 3*(1), e1387.

Goubet, F., & Mohnen, D. (1999). Solubilization and partial characterization of homogalacturonan-methyltransferase from microsomal membranes of suspension-cultured tobacco cells. *Plant Physiology, 121*(1), 281-290. Retrieved from https://www.ncbi.nlm.nih.gov/pmc/articles/PMC59378/pdf/281.pdf

Guex, N., Peitsch, M. C., & Schwede, T. (2009). Automated comparative protein structure modeling with SWISS-MODEL and Swiss-PdbViewer: A historical perspective. *Electrophoresis, 30*(S1), S162-S173.

Haigler, C., & Brown, R. (1986). Transport of rosettes from the Golgi apparatus to the plasma membrane in isolated mesophyll cells ofZinnia elegans during differentiation to tracheary elements in suspension culture. *Protoplasma, 134*(2-3), 111-120.

Hayashi, T. (1989). Xyloglucans in the primary cell wall. *Annual Review of Plant Biology, 40*(1), 139-168.

He, Z.-H., Cheeseman, I., He, D., & Kohorn, B. D. (1999). A cluster of five cell wall-associated receptor kinase genes, Wak1–5, are expressed in specific organs of Arabidopsis. *Plant Molecular Biology, 39*(6), 1189-1196. doi:10.1023/A:1006197318246

Herger, A., Dünser, K., Kleine-Vehn, J., & Ringli, C. (2019). Leucine-rich repeat extensin proteins and their role in cell wall sensing. *Current Biology, 29*(17), R851-R858.

Hothorn, M., Wolf, S., Aloy, P., Greiner, S., & Scheffzek, K. (2004). Structural insights into the target specificity of plant invertase and pectin methylesterase inhibitory proteins. *The Plant Cell, 16*(12), 3437-3447. Retrieved from https://www.ncbi.nlm.nih.gov/pmc/articles/PMC535884/pdf/tpc1603437.pdf

Jacob-Wilk, D., Kurek, I., Hogan, P., & Delmer, D. P. (2006). The cotton fiber zinc-binding domain of cellulose synthase A1 from Gossypium hirsutum displays rapid turnover in vitro and in vivo. *Proceedings of the National Academy of Sciences, 103*(32), 12191-12196. Retrieved from https://www.ncbi.nlm.nih.gov/pmc/articles/PMC1567717/pdf/zpq12191.pdf

Jarvis, M., Briggs, S., & Knox, J. (2003). Intercellular adhesion and cell separation in plants. *Plant, Cell & Environment, 26*(7), 977-989.

Keegstra, K. (2010). Plant cell walls. *Plant Physiology, 154*(2), 483-486. Retrieved from https://www.ncbi.nlm.nih.gov/pmc/articles/PMC2949028/pdf/483.pdf

Kohorn, B. D. (2015). Cell wall-associated kinases and pectin perception. *Journal of Experimental Botany, 67*(2), 489-494. doi:10.1093/jxb/erv467

Kohorn, B. D., Greed, B., Verger, S., Mouille, G., & Kohorn, S. (2021). Effects Of Arabidopsis Wall Associated Kinase Mutations On ESMERALDA1 And Elicitor Induced ROS. *PLoS One*.

Kohorn, B. D., Johansen, S., Shishido, A., Todorova, T., Martinez, R., Defeo, E., & Obregon, P. (2009). Pectin activation of MAP kinase and gene expression is WAK2 dependent. *The Plant Journal, 60*(6), 974-982. Retrieved from https://www.ncbi.nlm.nih.gov/pmc/articles/PMC3575133/pdf/nihms435147.pdf

Kohorn, B. D., Kobayashi, M., Johansen, S., Riese, J., Huang, L. F., Koch, K., . . . Byers, N. (2006). An Arabidopsis cell wall-associated kinase required for invertase activity and cell growth. *The Plant Journal, 46*(2), 307-316. Retrieved from https://onlinelibrary.wiley.com/doi/full/10.1111/j.1365-313X.2006.02695.x

Kohorn, B. D., & Kohorn, S. L. (2012). The cell wall-associated kinases, WAKs, as pectin receptors. *Frontiers in Plant Science, 3*, 88. Retrieved from https://www.ncbi.nlm.nih.gov/pmc/articles/PMC3355716/pdf/fpls-03-00088.pdf

Kohorn, B. D., Zorensky, F. D. H., Dexter-Meldrum, J., Chabout, S., Mouille, G., & Kohorn, S. (2021). Mutation of an arabidopsis golgi membrane protein ELMO1 reduces cell adhesion. *Development*. doi:10.1242/dev.199420

Liberman, M., Mutaftschiev, S., Jauneau, A., Vian, B., Catesson, A., & Goldberg, R. (1999). Mung bean hypocotyl homogalacturonan: localization, organization and origin. *Annals of Botany, 84*(2), 225-233.

Lionetti, V., Cervone, F., & De Lorenzo, G. (2015). A lower content of de-methylesterified homogalacturonan improves enzymatic cell separation and isolation of mesophyll protoplasts in Arabidopsis. *Phytochemistry, 112*, 188-194.

Liu, N., Sun, Y., Pei, Y., Zhang, X., Wang, P., Li, X., . . . Hou, Y. (2018). A pectin methylesterase inhibitor enhances resistance to Verticillium wilt. *Plant Physiology, 176*(3), 2202-2220. Retrieved from http://www.plantphysiol.org/content/plantphysiol/176/3/2202.full.pdf

Mouille, G., Ralet, M. C., Cavelier, C., Eland, C., Effroy, D., Hématy, K., . . . Thibault, J. F. (2007). Homogalacturonan synthesis in Arabidopsis thaliana requires a Golgi-localized protein with a putative methyltransferase domain. *The Plant Journal, 50*(4), 605-614. Retrieved from https://onlinelibrary.wiley.com/doi/full/10.1111/j.1365-313X.2007.03086.x

Neumetzler, L., Humphrey, T., Lumba, S., Snyder, S., Yeats, T. H., Usadel, B., . . . Persson, S. (2012). The FRIABLE1 gene product affects cell adhesion in Arabidopsis. *PLoS One, 7*(8), e42914. Retrieved from https://www.ncbi.nlm.nih.gov/pmc/articles/PMC3419242/pdf/pone.0042914.pdf

O'Neill, M. A., Warrenfeltz, D., Kates, K., Pellerin, P., Doco, T., Darvill, A. G., & Albersheim, P. (1996). Rhamnogalacturonan-II, A Pectic Polysaccharide in The Walls of Growing Plant Cell, Forms a Dimer That Is Covalently Cross-linked by a Borate Ester: *in vitro* Conditions for the Formation and Hydrolysis of the Dimer. *Journal of Biological Chemistry, 271*(37), 22923-22930.

Park, Y. B., & Cosgrove, D. J. (2015). Xyloglucan and its Interactions with Other Components of the Growing Cell Wall. *Plant and Cell Physiology, 56*(2), 180-194. doi:10.1093/pcp/pcu204

Perrin, R. M., Jia, Z., Wagner, T. A., O'Neill, M. A., Sarria, R., York, W. S., . . . Keegstra, K. (2003). Analysis of xyloglucan fucosylation in Arabidopsis. *Plant Physiology, 132*(2), 768-778. Retrieved from https://www.ncbi.nlm.nih.gov/pmc/articles/PMC167016/pdf/1320768.pdf

Seifert, G. J., & Roberts, K. (2007). The biology of arabinogalactan proteins. *Annual Review of Plant Biology, 58*, 137-161.

Sénéchal, F., Wattier, C., Rustérucci, C., & Pelloux, J. (2014). Homogalacturonan-modifying enzymes: structure, expression, and roles in plants. *Journal of Experimental Botany, 65*(18), 5125-5160. doi:10.1093/jxb/eru272

Showalter, A. M., & Basu, D. (2016). Extensin and arabinogalactan-protein biosynthesis: glycosyltransferases, research challenges, and biosensors. *Frontiers in Plant Science, 7*, 814. Retrieved from https://www.ncbi.nlm.nih.gov/pmc/articles/PMC4908140/pdf/fpls-07-00814.pdf

Steele, N. M., McCann, M. C., & Roberts, K. (1997). Pectin modification in cell walls of ripening tomatoes occurs in distinct domains. *Plant Physiology, 114*(1), 373-381. Retrieved from http://www.plantphysiol.org/content/plantphysiol/114/1/373.full.pdf

Studer, G., Rempfer, C., Waterhouse, A. M., Gumienny, R., Haas, J., & Schwede, T. (2020). QMEANDisCo—distance constraints applied on model quality estimation. *Bioinformatics, 36*(6), 1765-1771. Retrieved from https://www.ncbi.nlm.nih.gov/pmc/articles/PMC7075525/pdf/btz828.pdf

Thibault, J.-F., Renard, C. M., Axelos, M. A., Roger, P., & Crépeau, M.-J. (1993). Studies of the length of homogalacturonic regions in pectins by acid hydrolysis. *Carbohydrate Research, 238*, 271-286.

Verger, S., Chabout, S., Gineau, E., & Mouille, G. (2016). Cell adhesion in plants is under the control of putative O-fucosyltransferases. *Development, 143*(14), 2536-2540. Retrieved from https://dev.biologists.org/content/develop/143/14/2536.full.pdf

Watanabe, Y., Meents, M., McDonnell, L., Barkwill, S., Sampathkumar, A., Cartwright, H., . . . Mansfield, S. (2015). Visualization of cellulose synthases in Arabidopsis secondary cell walls. *Science, 350*(6257), 198-203. Retrieved from https://science.sciencemag.org/content/sci/350/6257/198.full.pdf

Waterhouse, A., Bertoni, M., Bienert, S., Studer, G., Tauriello, G., Gumienny, R., . . . Bordoli, L. (2018). SWISS-MODEL: homology modelling of protein structures and complexes. *Nucleic Acids Research, 46*(W1), W296-W303. Retrieved from https://www.ncbi.nlm.nih.gov/pmc/articles/PMC6030848/pdf/gky427.pdf

Wen, F., Zhu, Y., & Hawes, M. C. (1999). Effect of Pectin Methylesterase Gene Expression on Pea Root Development. *The Plant Cell, 11*(6), 1129-1140. doi:10.1105/tpc.11.6.1129

Willats, W. G., McCartney, L., Mackie, W., & Knox, J. P. (2001). Pectin: cell biology and prospects for functional analysis. *Plant Molecular Biology, 47*(1-2), 9-27.

Wolf, S., Mouille, G., & Pelloux, J. (2009). Homogalacturonan methyl-esterification and plant development. *Molecular Plant, 2*(5), 851-860.

Wormit, A., & Usadel, B. (2018). The multifaceted role of pectin methylesterase inhibitors (PMEIs). *International Journal of Molecular Sciences, 19*(10), 2878.

Xiao, C., Somerville, C., & Anderson, C. T. (2014). POLYGALACTURONASE INVOLVED IN EXPANSION1 functions in cell elongation and flower development in Arabidopsis. *Plant Cell, 26*(3), 1018-1035. Retrieved from https://escholarship.org/content/qt1tv7v2sk/qt1tv7v2sk.pdf?t=nyjblt

Zamil, M., & Geitmann, A. (2017). The middle lamella—more than a glue. *Physical Biology, 14*(1), 015004. Retrieved from https://iopscience.iop.org/article/10.1088/1478-3975/aa5ba5